

Supplementary Material for “Quantitative Estimates of the Volatility of Ambient Organic Aerosol”

Christopher D. Cappa¹ and Jose L. Jimenez²

[1] Department of Civil and Environmental Engineering, University of California, Davis, CA

[2] Cooperative Institute for Research in the Environmental Sciences (CIRES), and Department of Chemistry and Biochemistry, University of Colorado, Boulder, CO

Correspondence to: C. D. Cappa (cdcappa@ucdavis.edu)

SI-1: Modification of the Epstein et al. ΔH_{vap} vs. C^* Relationship

Epstein et al. have recently proposed a semi-empirical relationship between ΔH_{vap} and C^* (the effective saturation concentration), given as (Epstein et al., 2009)

$$\Delta H_{vap} = 131 - 11 \log(C^*). \quad (1.)$$

From this, we see that ΔH_{vap} increases with decreasing C^* values (at 25°C). Recalling the ΔH_{vap} describes the sensitivity of C^* to temperature, this indicates that the low C^* components will exhibit a greater sensitivity to changes in temperature than the high C^* components. A result of this is that when the Epstein et al. relationship is used without modification, the ΔH_{vap} values of the lowest C^* components are so large and the C^* values vary with temperature so dramatically that it is not possible to select a component with a low enough $C^*(25^\circ\text{C})$ value to still predict that any OA mass remains above $\sim 200^\circ\text{C}$ (see Figure S1). As such, we have modified the Epstein et al. relationship to have an upper-limit ΔH_{vap} of 200 kJ/mol. This upper-limit was selected so as to be generally consistent with the high ΔH_{vap} values determined for low volatility dicarboxylic acids (Cappa et al., 2007), where a value of 181 kJ/mol was observed for sebacic acid (a 10-carbon dicarboxylic acid). If a smaller value is chosen for this upper-limit on ΔH_{vap} , the result is that the required C^*_{min} increases and fewer overall bins are therefore required in the derived volatility distribution.

SI-2: Determining a Volatility Distribution from the Faulhaber et al. Relationship

A volatility distribution for the MILAGRO campaign average OA has been deduced using the empirical relationship introduced by Faulhaber et al. (2009). To do this, the observed mass thermogram (Huffman et al., 2009) was first linearly interpolated onto the temperature scale from the Faulhaber et al. T_{50}/C^* relationship using the equation

$$T_{50}^{-1} = \left(\log C^* + 23.61 + \log \left[\frac{R \times 298.15K}{MW} \right] \right) / 8171, \quad (2.)$$

where R is the ideal gas constant and where we have used logarithmically spaced C^* bins (and assumed $MW = 200$ g/mol). The organic aerosol mass required to give the observed mass fraction remaining (assuming a total $C_{OA} = 17$ $\mu\text{g}/\text{m}^3$) at each temperature is then iteratively

determined, starting from the highest temperatures (where the *MFR* is smallest) and going to the lowest temperatures (where the *MFR* goes to 1). The total organic mass (gas + aerosol) that will give the required OA mass in each been is then determined. Note that the thus determined C_{tot} vs. C^* distribution generally follows the exponential form assumed in the main text. A fit to the derived distribution gives $C_{i,tot} = 1.07 + 28\exp[1.37(\log(C^*) - 3)]$.

SI-3: Defining “globally” non-volatile material

Here, we start with the volatility distributions determined for the Mexico City average OA for the various ΔH_{vap} cases in section 3.1 of the main text. A global definition of non-volatile material is derived by taking these distributions (where $C_{OA} = 17 \text{ }\mu\text{g}/\text{m}^3$ at 25°C) and diluting until $C_{OA} = 0.1 \text{ }\mu\text{g}/\text{m}^3$ at 40°C . The resulting distributions of $C_{i,OA}$ are shown in Figure S2 and are compared to the initial distribution, divided by the dilution factor required to go from $17 \text{ }\mu\text{g}/\text{m}^3$ to $0.1 \text{ }\mu\text{g}/\text{m}^3$. This allows for simultaneous assessment of the influences of evaporation (from dilution) and temperature. From this, we see that for components which have $C^* \leq 10^{-3} \text{ }\mu\text{g}/\text{m}^3$ the absolute abundance of these components is essentially unchanged from the initial case (i.e. neither dilution nor temperature has a significant influence on their abundance, Figure S2). As such, we conclude that compounds that have C^* values $\leq 10^{-3} \text{ }\mu\text{g}/\text{m}^3$ will remain in the particle phase for the vast majority of conditions experienced on in the Earth’s atmosphere and thus we term these “globally” non-volatile. Note that had we chosen a lower value for the minimum C_{OA} (e.g. $10^{-3} \text{ }\mu\text{g}/\text{m}^3$ rather than $0.1 \text{ }\mu\text{g}/\text{m}^3$) the C^* below which components could be considered globally non-volatile would decrease.

SI-4: Alternative volatility distributions for LV-OOA

In addition to the exponential relationship between the total organics concentration, C_{tot} , and C^* presented in the main text, we have found that both a constant and a linear relationship can provide reasonable model/measurement agreement. For the constant C_{tot} vs. C^* relationship, we find that assuming $C_{i,tot} = 0.95 \text{ }\mu\text{g}/\text{m}^3$ with an upper limit of $C^* = 1 \text{ }\mu\text{g}/\text{m}^3$ and a lower limit of $C^* = 10^{-17} \text{ }\mu\text{g}/\text{m}^3$ provides reasonable agreement. For the linear relationship, we find that $C_{tot} = 0.53 - 0.2 \log(C^*)$ with an upper limit of $C^* = 100 \text{ }\mu\text{g}/\text{m}^3$ and a lower limit of $C^* = 10^{-10} \text{ }\mu\text{g}/\text{m}^3$ provides reasonable agreement. Note that the C_{min}^* value is not the same for the different

relationships considered, with C^*_{min} equal to 10^{-17} , 10^{-10} and 10^{-7} for the constant, linear and exponential relationships, respectively. That a lower C^*_{min} is required for e.g. the assumed constant vs. exponential relationship is the primary reason that there is little difference in the calculated globally non-volatile fraction, sensitivity to dilution and C^g_{SVOC} for the different assumptions. Volatility distributions and the associated calculated mass thermograms for each assumed relationship are shown in Figure S4. The globally non-volatile fraction, $f_{nv,g}$, is 0.88, 0.86 and 0.84 for the assumed exponential, linear and constant relationships, respectively.

SI-5: Calculations for $\gamma_e = 0.01$

As with the $\gamma_e = 1$ and $\gamma_e = 0.1$ cases discussed in the main text, we have also attempted to determine volatility distributions that provide for good model/measurement agreement when it is assumed that $\gamma_e = 0.01$. Recent measurements of the time-response of laboratory generated SOA and POA to dilution were interpreted as indicating that OA evaporates slowly, with an effective evaporation coefficient of < 0.01 (Grieshop et al., 2007; Grieshop et al., 2009). In this case, it was found that it is not possible to determine a volatility distribution that could match the observations over the entire temperature range (Figure S5). In particular, the discrepancy between model and measurement was found to be largest at low temperatures (50-75°C). The thermodenuder measurements fundamentally probe the kinetics of evaporation and not (necessarily) the ultimate equilibrium state. As such, this result can be understood as the high volatility components (e.g. $C^* \geq 10 \mu\text{g}/\text{m}^3$) not evaporating fast enough in the thermodenuder. The model/measurement disagreement is greatest for the lower ΔH_{vap} cases, but is still apparent in e.g. the variable ΔH_{vap} case. These results therefore indicate that the evaporation coefficient for ambient OA is > 0.01 .

SI References

- Cappa, C. D., Lovejoy, E. R., and Ravishankara, A. R.: Determination of Evaporation Rates and Vapor Pressures of Very Low Volatility Compounds: A Study of the C₄-C₁₀ and C₁₂ Dicarboxylic Acids, J. Phys. Chem. A, 111, 3099-3109, 2007.

Epstein, S. A., Riipinen, I., and Donahue, N. M.: A Semiempirical Correlation between Enthalpy of Vaporization and Saturation Concentration for Organic Aerosol, *Environ. Sci. Technol.*, 44, 743-748, doi: 10.1021/es902497z, 2009.

Faulhaber, A. E., Thomas, B. M., Jimenez, J. L., Jayne, J. T., Worsnop, D., and Ziemann, P. J.: Characterization of a thermodenuderparticle beam mass spectrometer system for the study of organic aerosol volatility and composition, *Atmos. Meas. Tech.*, 2, 15-31, 2009.

Grieshop, A. P., Donahue, N. M., and Robinson, A. L.: Is the gas-particle partitioning in alpha-pinene secondary organic aerosol reversible?, *Geophys. Res. Lett.*, 34, L14810, 2007.

Grieshop, A. P., Miracolo, M. A., Donahue, N. M., and Robinson, A. L.: Constraining the Volatility Distribution and Gas-Particle Partitioning of Combustion Aerosols Using Isothermal Dilution and Thermodenuder Measurements, *Environ. Sci. Technol.*, 43, 4750-4756, doi: 10.1021/es8032378, 2009.

Huffman, J. A., Docherty, K. S., Aiken, A. C., Cubison, M. J., Ulbrich, I. M., DeCarlo, P. F., Sueper, D., Jayne, J. T., Worsnop, D., Ziemann, P. J., and Jimenez, J. L.: Chemically-Resolved volatility measurements from two megacity field studies, *Atmos. Chem. Phys.*, 9, 7161-7182, 2009.

SI Figure Captions:

Figure S1. Model thermodenuder results using the Epstein et al. relationship between ΔH_{vap} and C^* without modification. Here, it was assumed that the total organic mass in each C^* bin was $0.77 \mu\text{g}/\text{m}^3$, which gives a total $C_{OA} \sim 17 \mu\text{g}/\text{m}^3$. The C^* bins used range from $1000 \mu\text{g}/\text{m}^3$ to $10^{-20} \mu\text{g}/\text{m}^3$. The lines correspond to the behavior of each of the individual compounds comprising the aerosol and are colored by the C^* values (see color bar). Note that the mass remaining (as opposed to the mass fraction remaining) is shown.

Figure S2. Calculations of the globally non-volatile compounds. Results are shown for the various constant ΔH_{vap} cases and the variable ΔH_{vap} case. The blue bars correspond to the organic aerosol mass distribution at 25°C and with $C_{OA} = 17 \mu\text{g}/\text{m}^3$, divided by the dilution factor required to give $C_{OA} = 0.1 \mu\text{g}/\text{m}^3$. The red bars are the distributions after dilution and heating to 40°C . The gray lines (right axis) show the ratio between the OA at 25°C and at 40°C . Values close to 1 indicate that the aerosol component can be considered globally non-volatile. Note that for the 50 kJ/mol case, there is no aerosol remaining at 40°C . The dilution factors required were 48 (75 kJ/mol), 71 (50 kJ/mol), 89 (125 kJ/mol), 104 (150 kJ/mol) and 115 (variable ΔH_{vap}).

Figure S3. The calculated $T_{50,nv}$ for the various ΔH_{vap} cases, shown as a function of ΔH_{vap} . The solid line is an exponential fit. The dashed line shows the calculated $T_{50,nv}$ for the variable ΔH_{vap} assumption.

Figure S4. Different assumptions as to the form of the volatility distribution for LV-OOA that provide reasonable model/measurement agreement with respect to the mass thermogram for (a) the constant, (b) the linear and (c) the exponential assumption. (d) Calculated mass thermograms for LV-OOA assuming various functional relationships between C_{tot} and C^* : constant (dot-dash), linear (solid) and exponential (dotted).

Figure S5. Calculated mass fraction remaining for the various ΔH_{vap} cases when $\gamma_e = 0.01$ (lines) compared to the observations from Mexico City (circles).

Figure S6. The E_{loss} values (i.e. the additional mass loss due to evaporation after dilution) for the $\gamma_e = 1$ (solid lines) and $\gamma_e = 0.1$ (dashed lines) cases. Results are shown for the various ΔH_{vap} cases. See main text (section 3.5) for details.

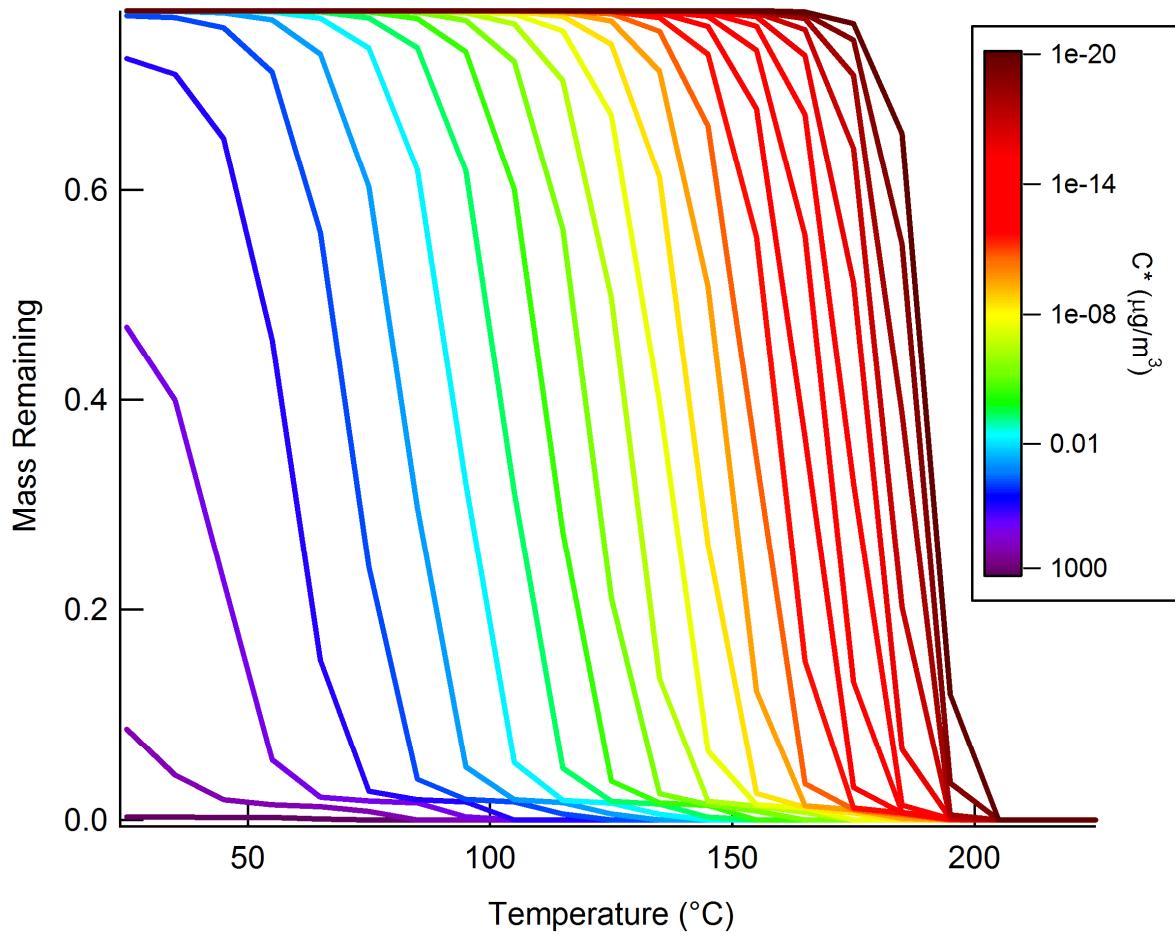


Figure S1.

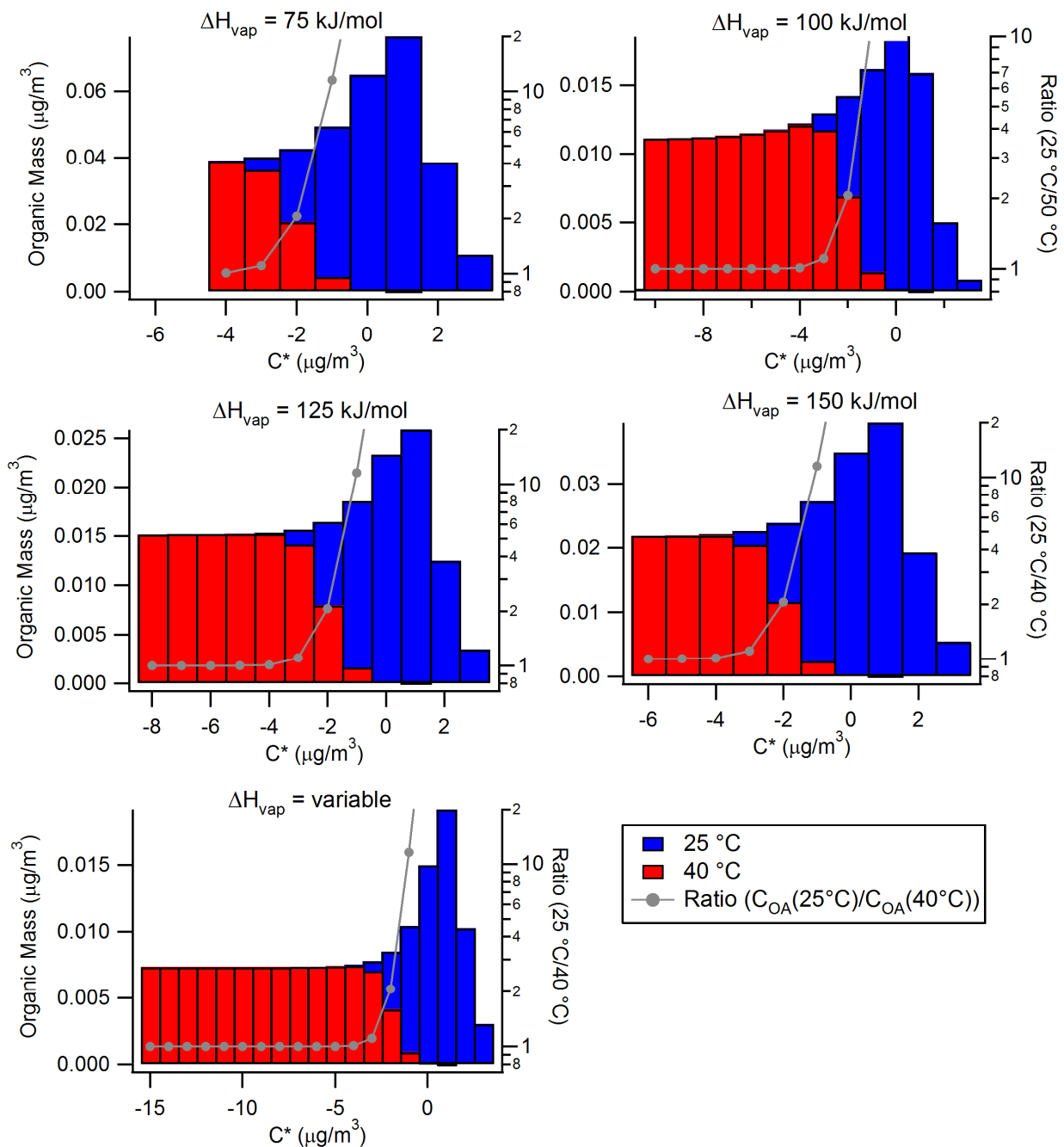


Figure S2.

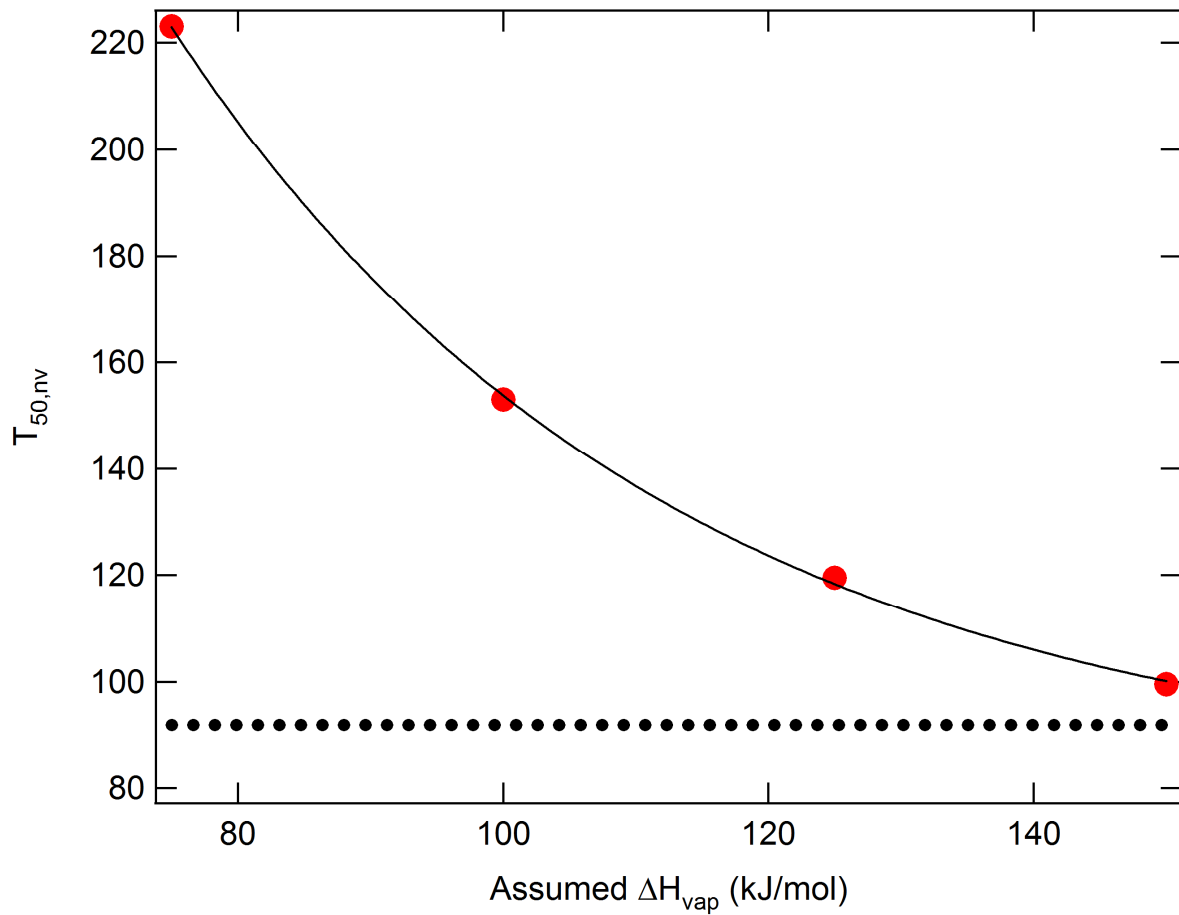


Figure S3.

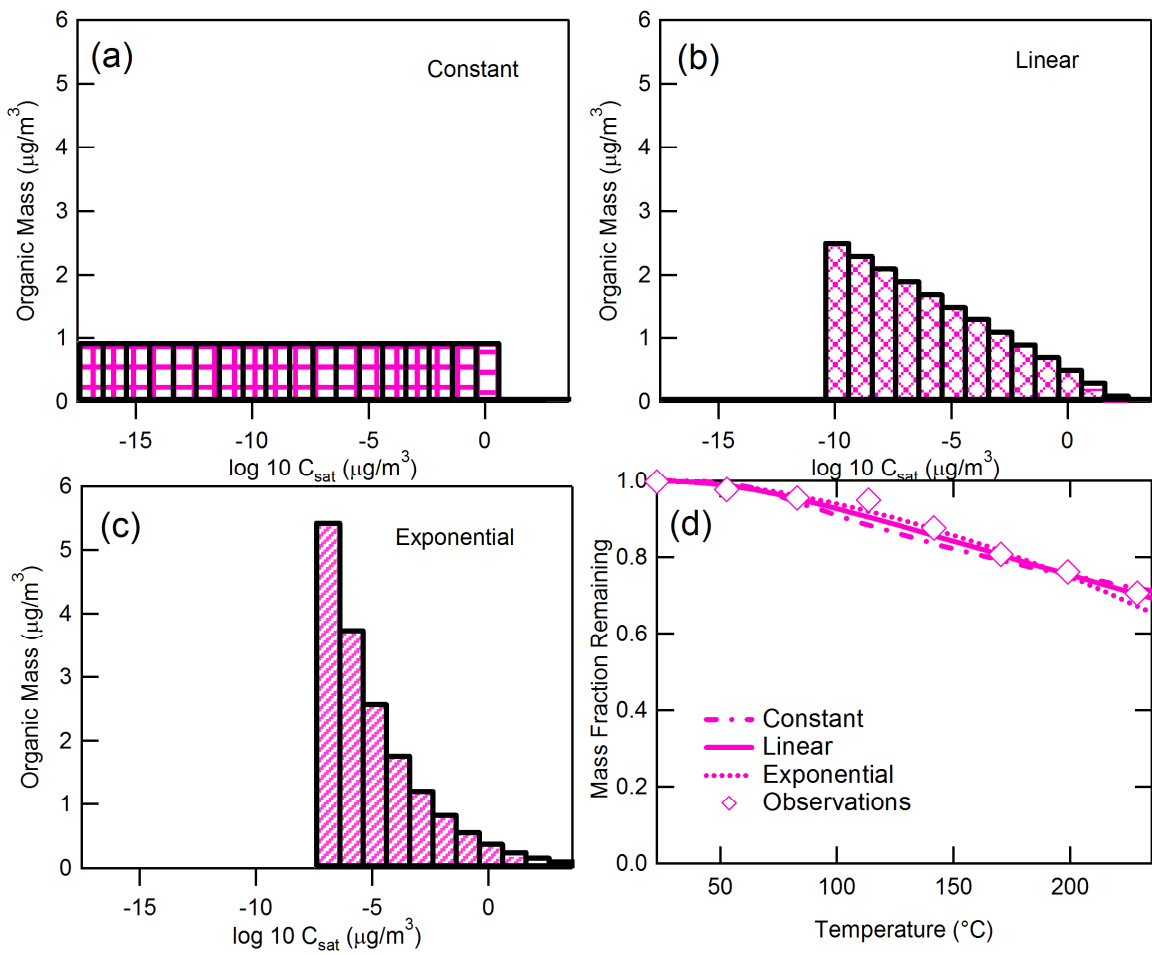


Figure S4.

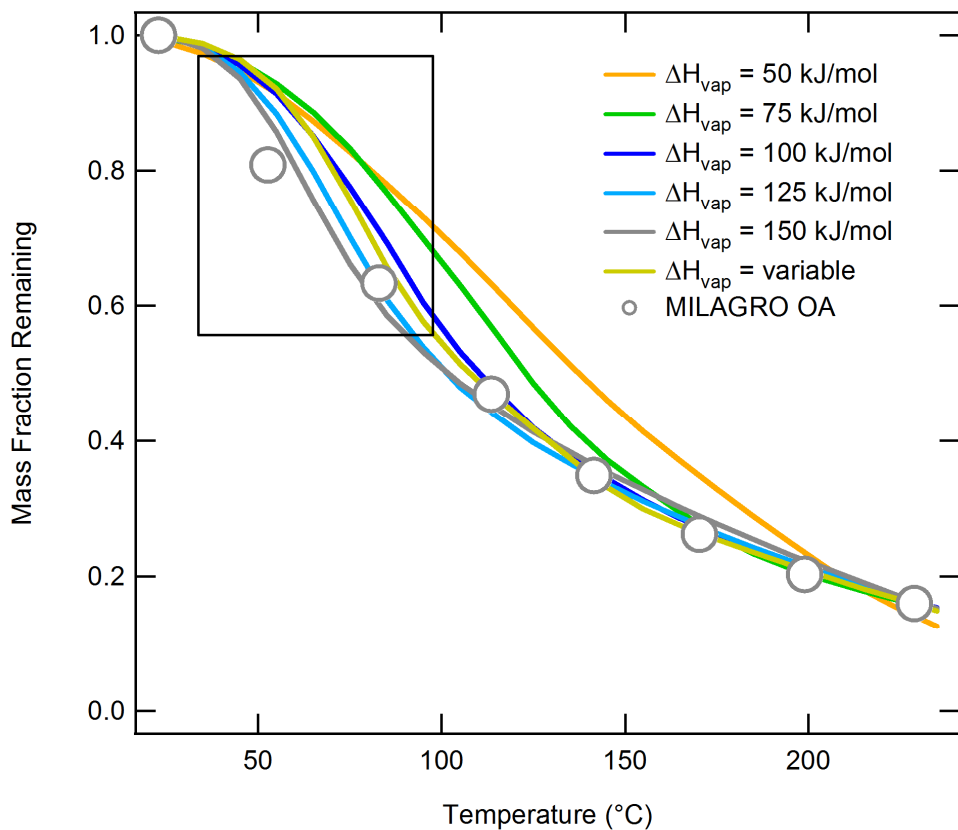


Figure S5.

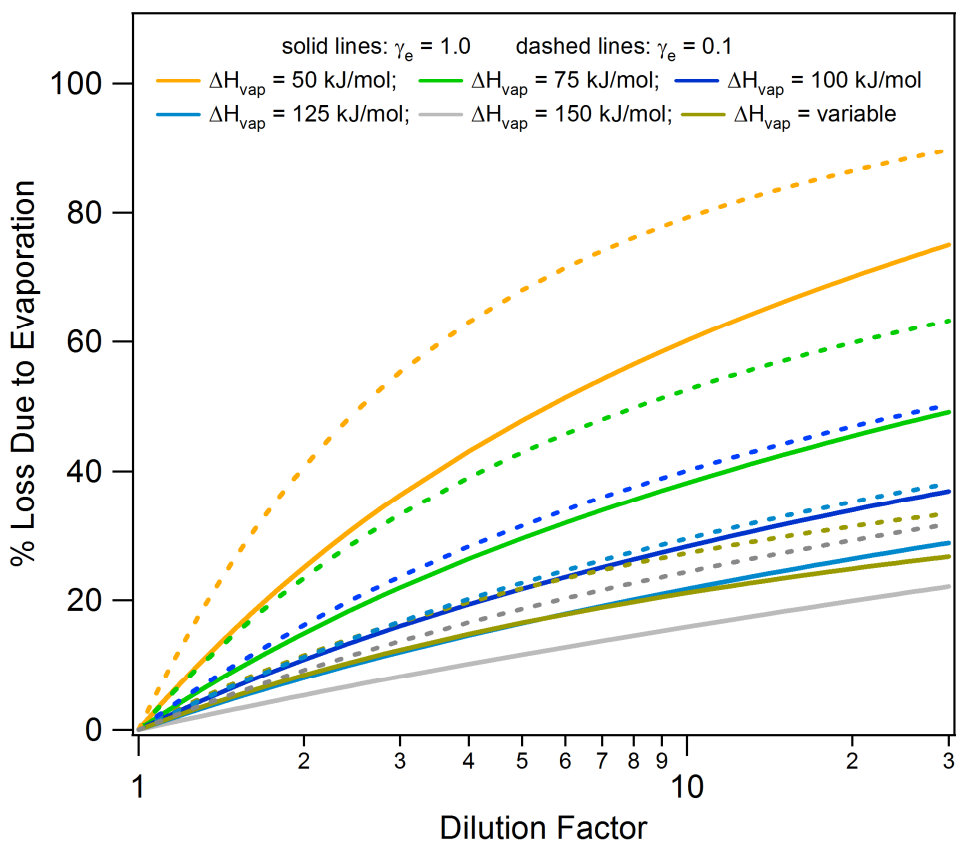


Figure S6.